

Article

Salt Weathering of 7th Century CE Granite Monument of Shore Temple, Mahabalipuram—Scientific Investigation and Conservation Strategy

S. Vinodh Kumar ¹ and M. R. Singh ^{2,*} 

¹ Archaeological Survey of India, Science Branch, Fort St. George, Chennai-600 009, India; vsvinodhkumar@gmail.com

² National Museum Institute, Department of Conservation, Janpath, New Delhi-110 011, India

* Correspondence: m_singh_asi@yahoo.com

† These authors contributed equally to this work.

Received: 11 October 2018; Accepted: 14 January 2019; Published: 17 January 2019



Abstract: Salt-induced deterioration of architectural heritage is accelerated drastically in marine environments. This paper investigates the deterioration mechanism of the Shore Temple using various analytical techniques. Deteriorated and pristine stone samples were analyzed using X-ray fluorescence spectroscopy (XRF), thin section studies, and SEM in order to understand the deterioration mechanism. The meteorological and micro-climatic conditions of Shore Temple in the tropical Indian climate were studied, as they have played a vital role in the deterioration of the stone matrix. The sides of the temple that face the sea as well as the upper part of the temple show intense alveolarization and the stone variety was petrologically identified as “garnetiferous hornblende biotite granite”. The evaluation of results in terms of the efficacy of ethyl silicate consolidation of stone after desalination is very difficult due to continuous sea sprays. The compatible lime rendering evidenced in the shelter area and then scientifically examined during this study may be applied as a protective layer to safeguard and conserve the lone Pallava edifice on the seashore from deterioration in tropical and hygric saline conditions.

Keywords: microclimatic conditions; poultice; lime plaster; granite; salt weathering; soluble salts; precipitation; relative humidity (RH); alveolarization

1. Introduction

Salt weathering is commonly noticed as one of the major factors in the deterioration of historical architecture, archaeological structures, and archaeological objects [1,2]. Marine salts and sand-laden winds are the permanent causes of natural pollution to historical buildings located near the coast. Higher precipitation and wind-driven rain may result in deeper penetration of sea salts in ancient structures that cause hygric expansion with accompanying stress [3]. High temperature, precipitation, and fluctuation in relative humidity are influencing climatic conditions that directly affect the salt weathering in porous building materials [4]. Salt weathering has long been known in porous materials [5] through the creation of physical stress from the crystallization of salts in pores [6,7]. Salts can damage stone and other building materials through a range of other mechanisms like differential thermal expansion, osmotic swelling of clays, crystallization pressure, hydration pressure, and enhanced wet/dry cycles caused by deliquescent salts [8–10]. Salt weathering refers to weathering generated by soluble and insoluble salts (such as in this study) and the weathering of salt [11].

The mechanical effect of salt weathering starts with crystallization pressure, which is the mechanism through which damage develops [12,13]. A particularly important feature is upscaling pressure from the pore scale to the material scale. Poromechanics [14–16] shows that the onset of macroscopic damage depends on crystallization pressure, the amount of salt accumulated, and properties of materials. Thus, the accumulation rates and localization of supersaturation, which depend on exposure conditions, play important roles as drivers for crystallization pressure. Analyzing salt damage involves transport kinetics, environmental exposure, materials chemistry, and poromechanics. Thomson [17] explained that tensile stress is produced in the matrix of a porous material when crystals grow in the pores. The tensile strength of the material should therefore be considered, and salts must propagate through a large enough fraction of the porous network to produce stress fields capable of propagating strength-limiting flaws (the largest defect in a material that is known to control its tensile strength) [18].

Salts contaminate the natural and artificial porous media in different ways. Salts can originate from incompatible building materials and inappropriate treatments, air pollution, de-icing treatments, and soil. Moisture and groundwater rising from foundations are other sources to consider. Some materials may even contain salts inherently. Salt deposition in buildings and monuments at coastal sites is mainly due to marine aerosol [19,20].

Stone containing salts often requires consolidation because salts are a common and powerful source of deterioration. This deterioration may take the forms of granular disintegration (powdering, sanding, etc.), scaling, flaking, and exfoliation, depending on the general and local concentration of the salts. As already mentioned, salts that have deliquesced properly may create a moisture or wetness problem that complicates treatment with alkoxysilanes. Stone in this condition should be dried slowly to reduce damage from crystallization. One of the goals of consolidation is to reduce losses during the removal of salts.

Alveolarization (honeycomb weathering) is a type of weathering of rocks and stones that is also known as stone lattice, stone lace, and fretting or alveolar weathering [21,22]. It is a common phenomenon among many rock surfaces with important implications in geomorphology, environmental geology, and stone conservation [23]. The alveolarization is mainly formed in coastal areas [24], in hot and cold deserts [25], and in some continental areas. This type of weathering is also found in many historical buildings constructed with various stone materials [26]. A previous study also reported the evidence of alveolarization on Mars [27]. The alveolarization is formed on stone surfaces that undergo periodic heavy spray and splash during stormy weather and are therefore regularly exposed to both wind and salt deposition. The loss of stone on historic buildings affected by alveolarization has been the concern of both conservators and researchers for a long time, who must understand its origins in order to develop mitigation methods. Alveolarization was noticed on three sides of the walls of the main Gopura of the Shore Temple (Figure 1).



Figure 1. Photograph showing the “alveolarization” in the south side main vimana of the Shore Temple.

Heritage Site

The Shore Temple, located in Mahabalipuram ($12^{\circ}36'59''$ N $80^{\circ}11'55''$ E) and attributed to the famous Pallava, who was the ruler of Narasimhavarman-II (722 CE), is one of the first stone temples in the South Indian Dravidian style. It was built with half of it in the sea and a half of it on land in the 7th–8th century CE [28]. The general view of the Shore Temple is shown in Figure 2. The paramount problem of this temple is its location. The location and plan map of the Shore Temple in Mahabalipuram is shown in Figure 3.



Figure 2. General view of Shore Temple, Mahabalipuram.

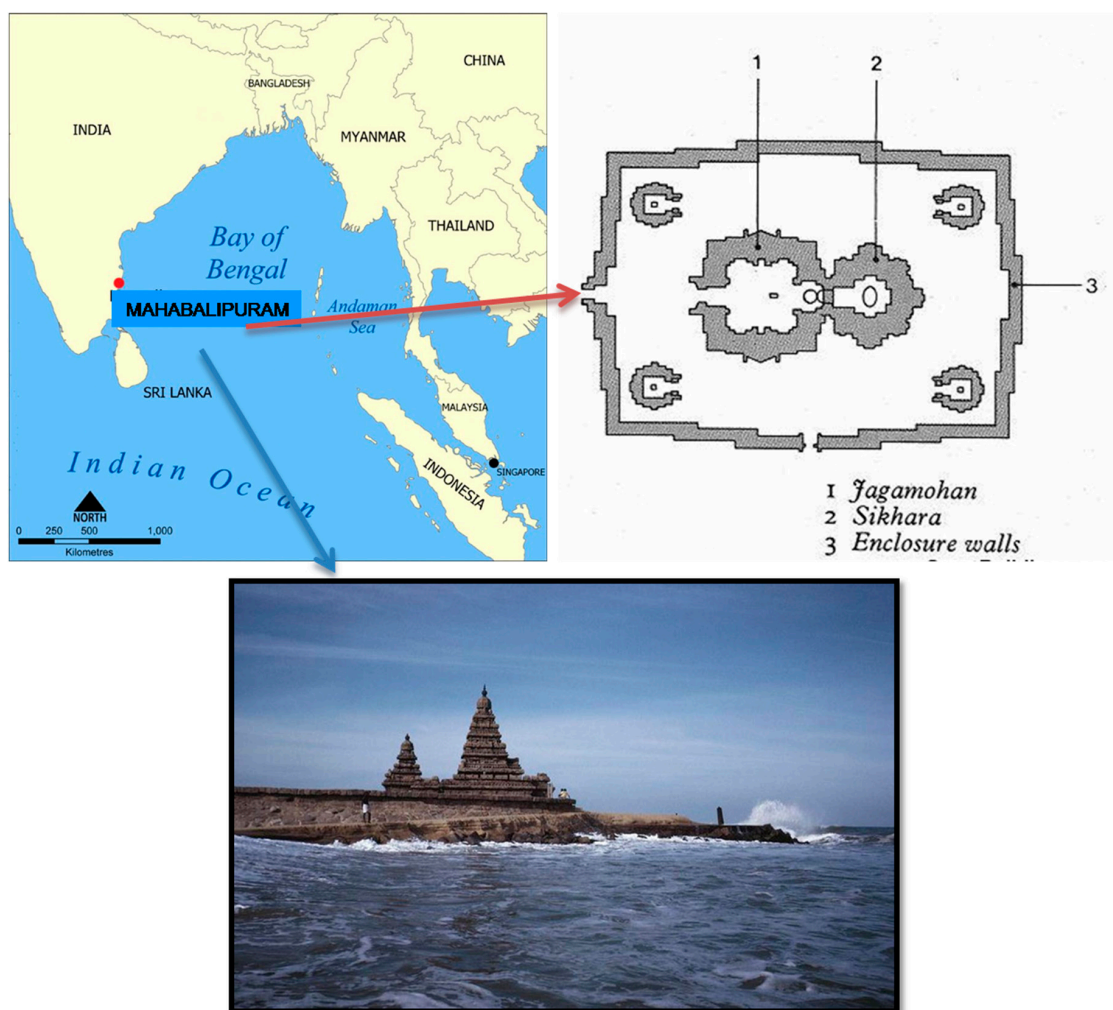


Figure 3. Location and plan map of Shore Temple, Mahabalipuram.

At Shore Temple, the side exposed directly to the sea was damaged to such an extent that sculptures were obliterated beyond recognition. The sculptures of the northern and the western sides were also damaged, but the profile remained. The extensive erosion observed on the upper part of the temple—about two meters from ground level—was probably due to the striking high-velocity winds. The loss of stone materials occurred in two ways. Firstly, morphological changes of the stone types due to partial/selective weathering, called relief, were noticed. This consisted of severe pitting on the stone surface due to the action of wind. In some places, alteration of gloss due to corrosion or loss of small stone particles from the stone surface was also observed. Secondly, soiling due to efflorescence (the formation of salty accretions due to efflorescence) was also observed on the stone monument. As the temple was constructed in granitic stone of different compositions and textures, the rate of deterioration was not the same in different stone blocks. The main weathering patterns observed were the color alteration, loss of cohesion, disaggregation, and detachment of the surface layer. The combined impact of high temperature and high precipitation also caused bio-colonization, which enhanced bio-deterioration. The deposition of bat excreta was observed, and a few bats were found roosting inside the ceiling of the interior portion of the temple. Due to high humidity, the guano has spread and contaminated the original stone surface. On the upper part of the temple, bird droppings were observed. The weathering by bird droppings seems to be an active factor of the structural and textural changes, as well as the deterioration in some of the stones, as evidenced by various researchers [29–32]. A conservation mapping of Shore Temple that shows different types of deterioration and discoloration/deposits is shown in Figure 4.

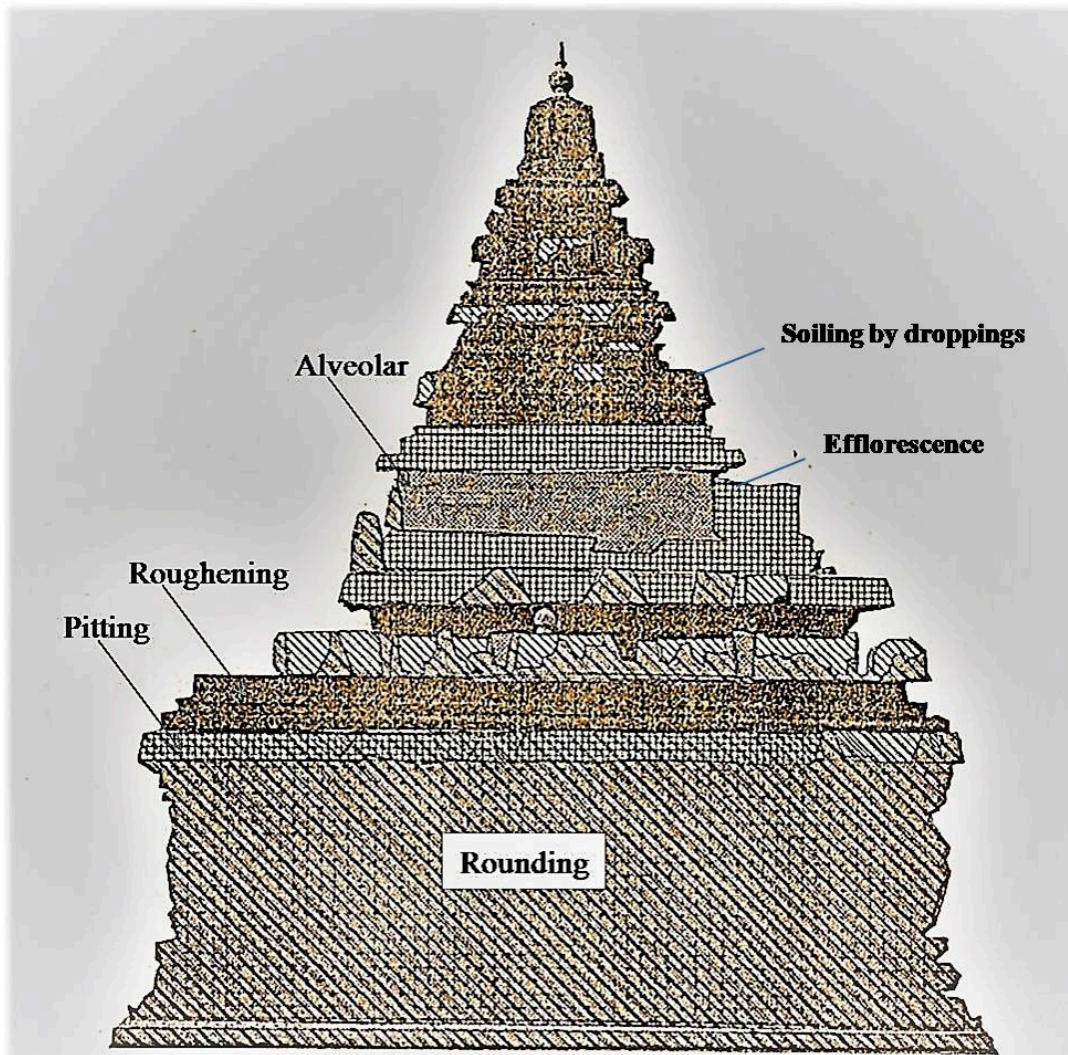


Figure 4. Conservation mapping of Shore Temple (southern side) showing the different types of deterioration and discoloration/deposits observed.

The deterioration of building materials induced by environmental factors is a complex interplay of the climatic effect and local meteorological parameters, biological processes, and complicated chemical processes resulting from the impact of pollutants and natural constituents from the surrounding environment. Climatic conditions and meteorological parameters can affect damaging processes in the form of mechanical stress, desiccation, surface scaling, attrition, and cracking, and may also accelerate certain forms of chemical attacks on the materials. The climate factors like air temperature, sunlight radiation, air humidity, different forms of precipitation (rain, snow, etc.), wind velocity, and direction are undoubtedly significant. The impact of these environmental parameters varies and depends on the sunshine, temperature fluctuations (rapid and large diurnal temperature changes), air movement/pressure, rain intensity, and frequency of local soil hydrology. The photograph shows the various types of deterioration noticed in Shore Temple (Figure 5).



Figure 5. The photograph shows the various types of deterioration noticed in Shore Temple.

The main aim of the paper is to suggest a suitable technique for the complete elimination of salt efflorescence and crypto efflorescence. This paper also studies the weathering of Shore Temple and the changes in the chemical composition of the stone matrix due to saline action and sandblast. The experimental results are based on the analysis of a few granite samples collected from different locations of Shore Temple in order to illustrate the deterioration of the stone. The environmental factors playing a vital role in the deterioration of the temple and the suitable conservation measures that need to be adopted in the future are elaborated vis-à-vis its efficacy in the present context.

2. Materials and Methods

The granite stone of the monument was visually examined at the site with the aid of a magnifying lens. Six of the stone samples obtained from the surface were used for analytical study and the data were compared with two of the sound samples extracted from deep inside the Vimana of the temple. The chemical analysis of the stone samples was carried with the help of Perkin-Elmer atomic absorption spectrophotometer Model PINAACLE900Z, as per the standard procedure of dissolving in suitable solvent mixtures. The loss on ignition (LOI) was determined at 900 °C in a muffle furnace. Remarkable variations were observed in the mineral constituents, and the internal structure of the sub-surface granite stone from the historical building was also examined. Further, detailed petrographic studies of the building material were also carried out with the help of a petrographic microscope in the laboratory of the Geological Survey of India, Hyderabad. Thin sections of the stone samples were prepared and analyzed with the help of a Carl Zeiss JENAPOL condenser polarizing microscope at various magnifications, and the data were recorded. The granite stone samples of the monument were also observed under high resolution SEM equipped with electron dispersive x-ray analysis (EDX) model FEI Quanta FEG-200 to understand the mineralogical composition of the rock and the deterioration of the monument stone. The measurement of the aqueous extract of the stone sample was carried out

with the Ion Analyzer (Orion 407A). The conductivity measurement was carried out by a conductivity analyzer (ELICO-M827).

Studied under a petrographic microscope were eight samples of granite stone chips from the temple, four from the Somaskanda panel facing west, three from the Somaskanda panel facing east, and one from Dhvajasthambha, which was near the concrete arch and close to the sea. This was done to evaluate the intensity of weathering at different locations of the monument.

From close inspection of the exterior and interior parts of the stone surface of the monument, it appeared that the monument was lime plastered in the past as a protective layer. All of the lime plaster layers were lost during the course of time, and traces remain on the inner sculpture and the shelter area (Figure 6). The lime plaster sample of the temple was subjected to particle size analysis with the help of an electronic particle size analyzer (Eye Tech particle size and shape analyzer, Ambivalu, Netherlands) to understand the distribution of grain size. The plaster sample was also analyzed with differential thermal analysis (DTA) and thermo gravimetric analysis (TGA), which was performed with the Mettler Toledo star thermal analyzer to study the purity of the plaster.

The conductivity of the water samples obtained from paper pulp application was measured by a standard method (ISO standard 7888:1985) [33]. The chloride estimation of water samples was carried out as per standard ISO 9297:2000 [34]. Standard NF ISO 9297 is based on the Mohr method. It uses a colorimetric determination of the equivalent point (with silver chromate). With the same titrant, it is possible to use a potentiometric determination of the equivalent point. The silver nitrate reacts with chloride ion according to:



This application uses a potentiometric titration with a combined silver/reference electrode and the equivalence point is detected using the inflection point mode.



Figure 6. Photograph showing the remnants of old lime plasters at Shore Temple, Mahabalipuram.

Environmental parameters around the temple have been recorded with the help of automatic weather station (AWS) installed by the Indian Space Research Organization (ISRO), Bengaluru.

The latitude and longitude of the exact location of the AWS installed is 12°37'2" N and 80°7'14" E, respectively. The AWS was installed in the temple complex at the same ground level as the temple. It records the temperature, relative humidity, precipitation data, wind speed, wind direction, sunshine, etc., and the data are downloaded through the satellite.

The salinity of the Indian ocean is about 34% [35]. Sodium is the most abundant cation of sea water. Chloride ions make up about 55% (by weight) of the dissolved material in the sea [36]. The high ionic strength of sea salts may accelerate the deterioration process of stone. Desalination of masonry is usually attempted through the use of poultices, which may consist of a range of materials (e.g., clay, sand, and paper pulp) [37]. Repeated application of paper pulp soaked in deionized water was carried out for extracting soluble salts from stone surfaces.

3. Results

3.1. Meteorological and Micro-Climatic Condition

Mahabalipuram has a tropical climate. In the winter, there is much less rainfall than in the summer. The Koppen–Geiger climate classified the site as Aw (tropical wet-dry climate) [38,39]. The climate is either classified as tropical wet-dry or tropical savanna climate. The drier months see precipitation totals less than 60 mm (2.4 in) and less than 4% of the total arrival precipitation. The average annual temperature in Mahabalipuram is 28.4 °C. In one year, the average rainfall is 1219 mm. The maximum temperature (upper brown line) for a year at Mahabalipuram is in the range of 28 °C to 41 °C (Figure 7a). Likewise, the average minimum temperature (lower brown line) for a year varies between 19 °C to 27 °C. The annual relative humidity (RH) at Mahabalipuram is in the range of 50% to 80% (shown in blue). However, the relative humidity recorded by the AWS installed in the temple complex varied between 31% to 98.97% in various seasons (Table 1). The precipitation diagram of Mahabalipuram (Figure 7b) shows the precipitation level during the months of January 2016 to December 2016. In Figure 7b, the cloudy days are shown in the grey background, and clear skies are shown with a yellow background. The darker the grey background, the denser the cloud cover. In tropical and monsoon climates, these amounts may be underestimated. The least amount of rainfall occurred in the period from January 2016 to April 2016. The most precipitation occurred during the months of June 2016 to December 2016, and the most remarkable changes were in the months of September 2016 to December 2016.

Table 1. Microclimatic data of Shore Temple, Mahabalipuram, recorded by automatic weather station (AWS).

Month	Temp in °C		Relative Humidity (%)		Rain Fall in mm	
	Max	Min	Max	Min	Max	Min
September 2008	37.07	22.07	98.97	44.92	246	165
October 2008	37.07	19.09	98.97	42.96	452	246
November 2008	32.97	17.67	98.97	44.65	450	350
December 2008	31.5	18.5	96.54	43.56	400	230
January 2009	29.5	21.32	92.91	61.35	-	-
February 2009	29.5	21.38	92.91	61.93	645	0
March 2009	31.45	22.56	92.91	48.92	653	0
April 2009	32.58	22.65	89.98	51.96	653	0
May 2009	36	23.29	89.98	37	670	0
June 2009	39.96	23	91.94	30.94	681	0
July 2009	39.96	22.26	93.99	61.35	55	-
August 2009	35.17	21.68	92.91	61.93	205	55

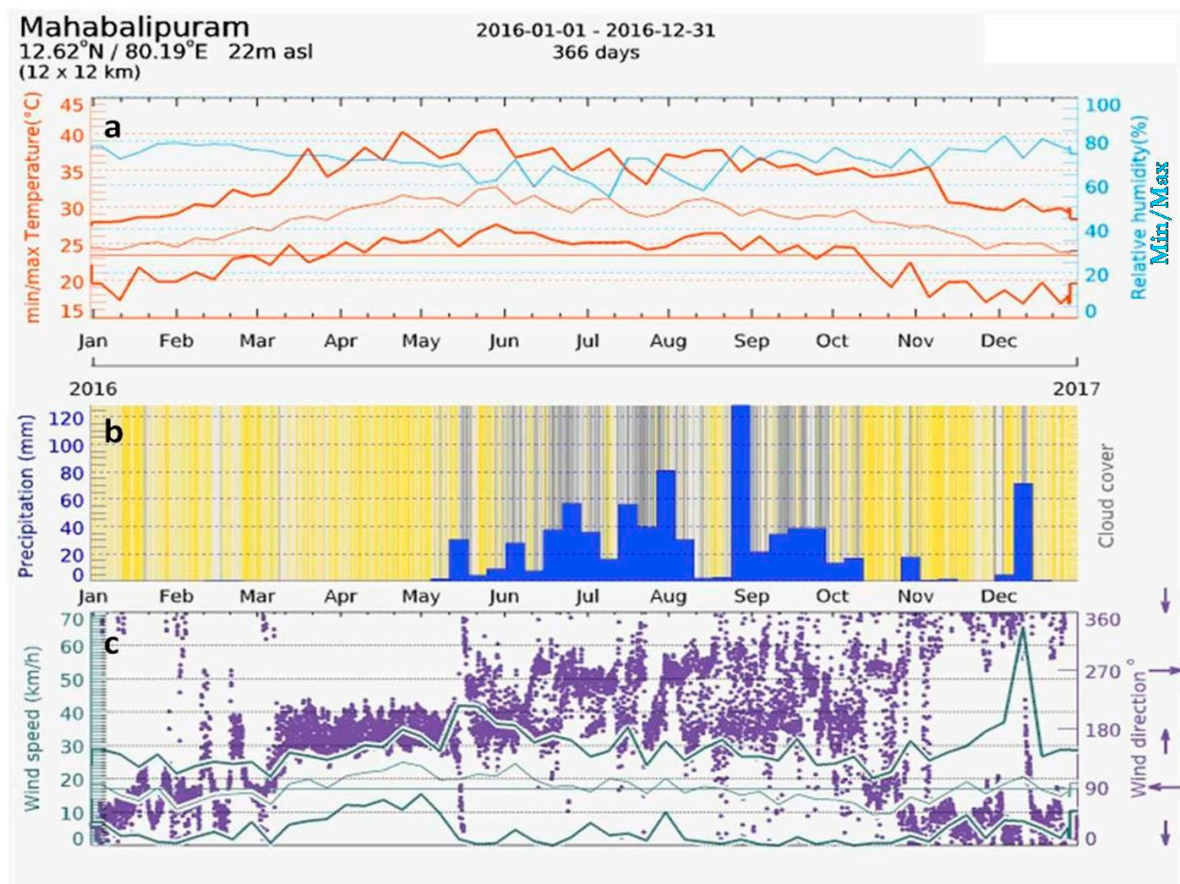


Figure 7. (a) Temperature and relative humidity versus time graph of Mahabalipuram; (b) precipitation diagram of Mahabalipuram; (c) graph showing the wind direction and wind speed at Mahabalipuram (derived from www.meteoblue.com).

Figure 7c shows the wind speed and wind direction at Mahabalipuram for a period from January 2016 to December 2016. The wind speed and direction was, in degrees, 0° = north, 90° = east, 180° = south, and 270° = west. In the meteogram (Figure 7c), the purple points represent the wind direction, as indicated on the right axis. From the meteogram, it can be seen that the maximum wind flowing directions were in the order of south, west, and north, respectively. The three lines represent the maximum, minimum, and average wind speeds. As the temple is located on the seashore, the salt-laden wind from the sea—especially from the south, east, and north directions—strike the walls of Shore Temple, causing a major conservation threat to the temple. The direction of the wind is mainly south to west during rainy seasons, while in dry times with lower humidity, the winds flow from the north. This has implications in the material decay processes. The high relative humidity (more than 50%) also forms aerosols with the salt particles and deteriorates the stone surfaces of the Shore Temple [14,16]. The hot, humid, and salty environmental conditions are conservation perils to the Shore Temple.

3.2. Petrographic Analysis

The granite rock of Shore Temple, Mahabalipuram is dark grey and medium grain. It exhibits a hypidiomorphic granular texture with indistinct to well-developed foliation, which indicates metamorphic rocks. The minerals noticed under the petrographic microscope from the thin section image of the granite stone are shown in Figure 8 under various magnifications. The presence of major minerals like quartz, microcline, orthoclase, plagioclase, and brown biotite in minor quantity is observed from the petrographic images. Zircon and apatite are also seen in trace quantities in the

thin section. The hornblende observed in the thin section is a complex inosilicates series of mineral that easily alters to chlorite and epidote. Based on our results of the thin section images of the stone samples, the rock was identified as “garnetiferous hornblende biotite granite”. All of the minerals are seen approximately in the composition, as shown in Table 2.

Table 2. Mineral composition of the stone sample.

Minerals	Percentage
Microcline	About 60%
Quartz	About 20%
Plagioclase	About 8 %
Orthoclase	About 6 %
Biotite	About 2%

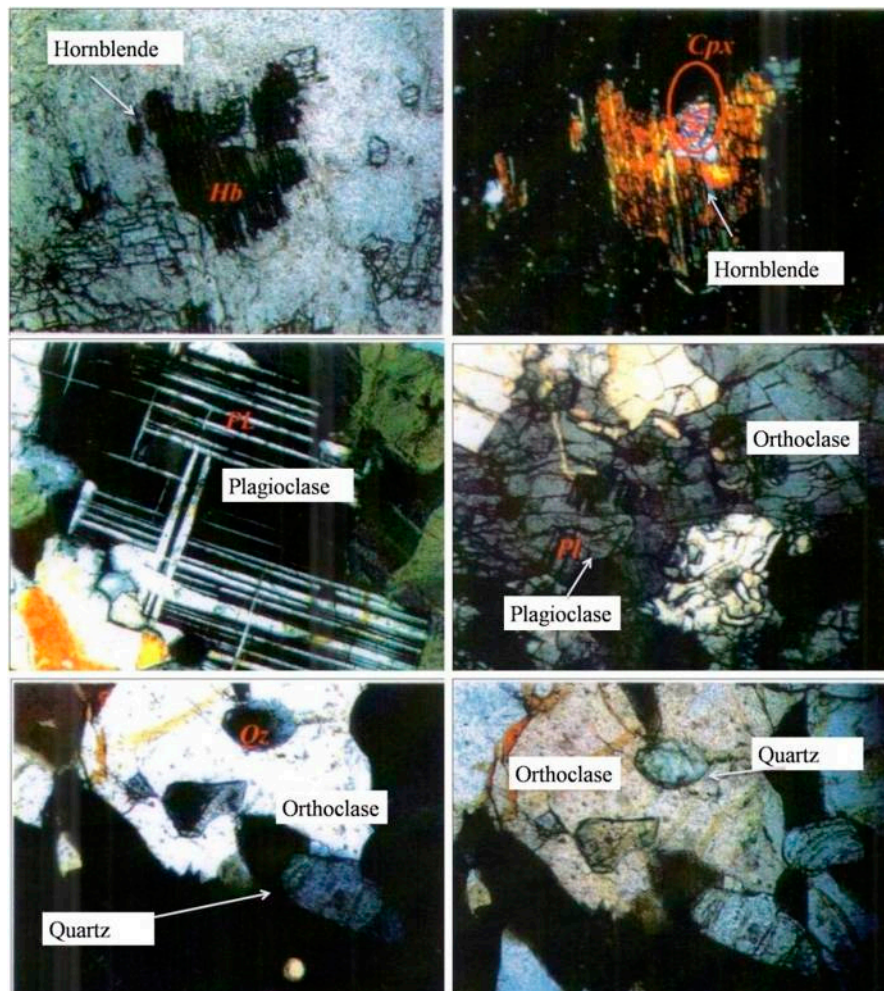


Figure 8. Thin section images of stone samples of Shore Temple, Mahabalipuram (Qz = Quartz, Pl = Plagioclase, Cpx = Clinopyroxene, Hb = Hornblende).

All of the felsic minerals—namely quartz, microcline, and plagioclase—broadly showed two size ranges, ranging from 0.05 mm to 0.07 mm and 0.02 mm to 0.25 mm. Slightly larger grains were seen in some samples, in which the grain size ranged from 0.05 mm to 0.15 mm.

From the petrographic examination, it was observed that biotite and feldspar altered at different degrees, increasing from west to east of the temple. The alteration may be attributed to weathering. The Dhvajasthamba near the sea indicated more alteration than that of the Somaskanda panel facing east. The erosion on the east side of the temple was comparatively worse than on the west side, mainly due to prevailing winds and direct exposure to the sea. It was observed that damage reached more than 1.5 m above ground level, and most of the damage observed was up to 7.5 m high on the temple.

3.3. Chemical Analyses

The alterations in the chemical composition due to saline action were investigated on six surface samples (samples 1–6), and the data were compared with two numbers of sound samples extracted from deep inside the temple (samples 7 and 8). Remarkable variations were observed in some of the mineral contents from the samples that were in a particularly deteriorated state (Table 3).

Table 3. Chemical composition of stone samples of Shore Temple, Mahabalipuram.

Sample No.	CaO	MgO	Al ₂ O ₃	SiO ₂	Fe ₂ O ₃	Na ₂ O	K ₂ O	TiO ₂	MnO	LOI *
Sample No.1	1.82	0.45	15.17	69.80	1.49	5.20	4.8	0.18	0.02	0.86
Sample No.2	1.82	0.56	16.73	67.05	1.71	5.90	4.08	0.17	0.02	0.78
Sample No.3	1.43	0.55	15.32	69.12	1.85	5.65	4.50	0.20	0.02	0.66
Sample No.4	1.55	0.51	15.01	70.71	0.88	5.18	4.71	0.13	0.01	0.68
Sample No.5	1.77	0.45	16.32	68.61	1.24	6.17	4.05	0.04	0.03	0.72
Sample No.6	1.69	0.52	15.24	72.56	2.37	4.65	4.40	0.07	0.09	1.03
Sample No.7	0.72	0.10	12.59	80.78	0.97	1.34	2.14	0.10	0.04	1.14
Sample No.8	0.84	0.22	12.26	75.89	1.32	2.45	3.61	0.13	0.03	0.05

* LOI = loss on ignition, samples 1–6 = weathered stone, samples 7 and 8 = pristine stone.

From the chemical analysis results, it was observed that SiO₂ and Al₂O₃ together constituted about 83.78% to 84.19% of the deteriorating stone. The relation between Al₂O₃ and SiO₂ was linear, showing an increase in the proportion of Al₂O₃ in the deteriorated samples with the corresponding decrease in SiO₂ percentage. Alumina was generally enriched in heavily deteriorated stones accompanied with higher depletion of SiO₂ [40]. The percentage of alumina (Al₂O₃) also indicated the sea sprays absorption capacity of weather stone [41]. The variation in the percentage of Fe₂O₃ and MnO noticed may have been due to deterioration [40]. The considerable deposits of salts observed on the surface were due to desiccation of seawater on the days when the atmospheric temperatures were high (35–40°). Crystal growth of salts is favored in large pores because the chemical potential of crystallization is inversely proportional to their radii [42]. The crystal growth in small pores can start only after the larger pores are completely filled. Due to the compact nature of granite rocks (porosity < 0.5%, derived from mercury porosimetry), most of the salt crystals were observed on the external surfaces. Silica in the form of quartz was almost insoluble, but other forms of silica were soluble—to a considerable degree—in the presence of alkaline carbonates. The preponderant salt is sodium chloride, which forms a white crystalline efflorescence at the surface. The same was observed in our SEM images. The sides exposed towards the sea showed high amounts of salt on the surface. The Na₂O and K₂O together constituted about 10% of granite rock. Samples enriched with Al₂O₃ also showed enrichment of Na₂O, denoting the role of alkali salts in the decay of less stable aluminosilicates. The potash aluminosilicates of the rock (representing the orthoclase and the microcline of the felspar group) was a mineral composed of a strong base and a weak acid, and was therefore very liable for hydrolysis. The principal results of hydrolysis were the removal of metals of the alkalies and alkaline earth, and the liberation and removal of silica in a soluble form. There was consequently a considerable concentration of alumina in the solid substance released by hydrolysis when compared to a sound sample. There was constant enrichment of alkali salts in the deteriorating stone at the temple due to marine salts pollution.

3.4. SEM-EDX of the Mahabalipuram Granite Stone

SEM-EDX of pristine samples (samples collected from the Vimana of the temple) and weathered granite stone are shown in Figures 9 and 10, respectively. From the SEM photomicrograph and EDX, the presence of authigenic K-feldspar overgrowths was observed. In SEM, these overgrowths appeared as small (2–10 μm) rhombic crystals (arrow). Identification of the authigenic mineral was based on EDX analysis and yielded the major elements Si, Al, and K. This was a typical EDX spectrum for K-feldspar. The presence of plagioclase feldspar with K-feldspar overgrowths was also seen as plagioclase feldspar grain partly covered with authigenic K-feldspar overgrowths. In Figure 9b, the isolated rhombic crystal was observed. The morphology of this grain was not distinctive in SEM. Thus, identification was based on the analysis of the major elements, as determined in the EDX analysis. The EDX spectrum indicated the presence of Si, Al, Ca, and Na, and their relative peak heights were consistent with the formula for plagioclase feldspar. The EDX spectrum (Figure 11) is shown as representative (not all the EDX spectra are shown). The overgrowths consisted of S, Al, and K, and the relative peak heights indicated K-feldspar. Elongated detrital (sand-size framework component together with any interstitial primary) biotite grain compacted between detrital quartz grains were also seen in the SEM photomicrograph. Individual cleavage planes of biotite appeared as flakes. Identification of mica as biotite was based on EDX analysis showing the major elements of biotite (Si, Al, Mg, K, Fe, and Ti).

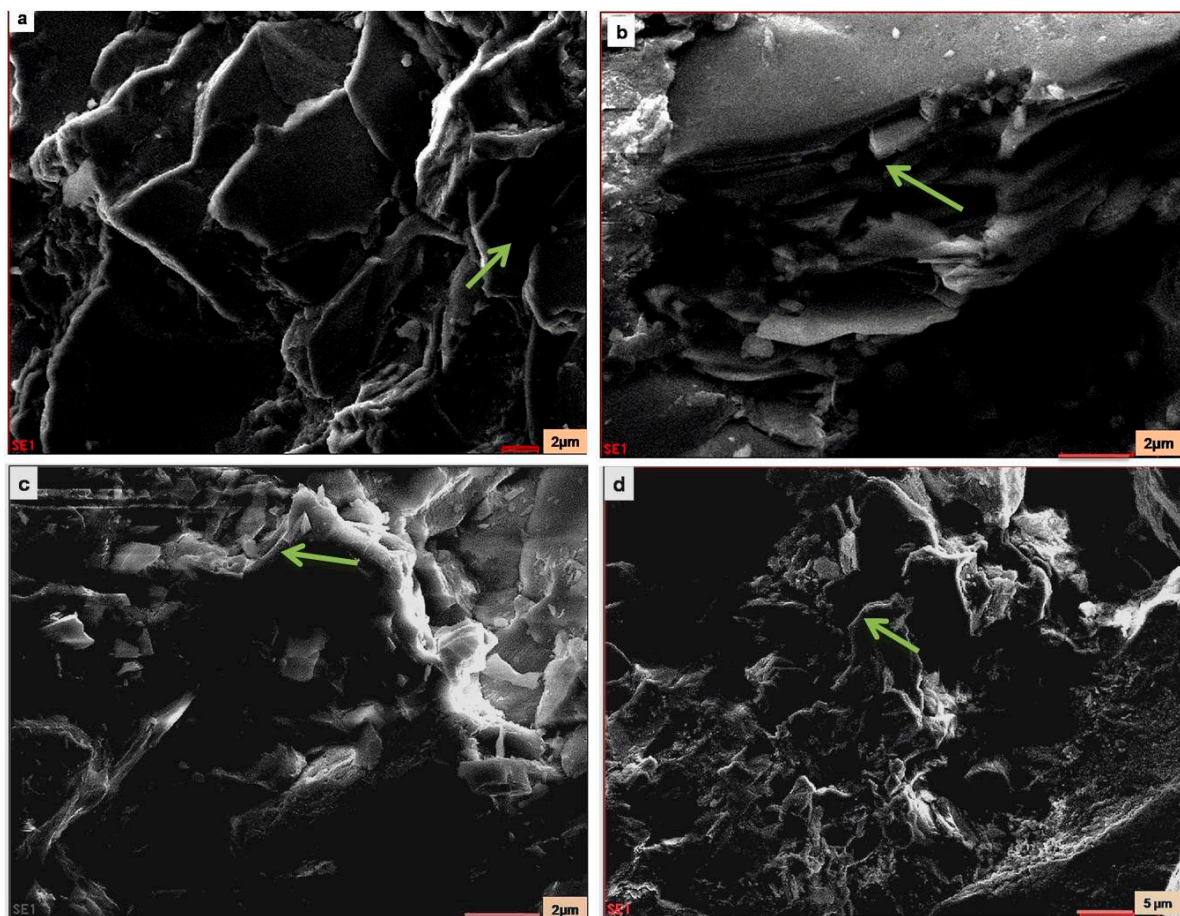


Figure 9. SEM images of the pristine stone sample: (a) arrow shows Mica–Biotite; (b) arrow shows K-feldspar and Mica; (c) arrow shows quartz; (d) arrow shows quartz.

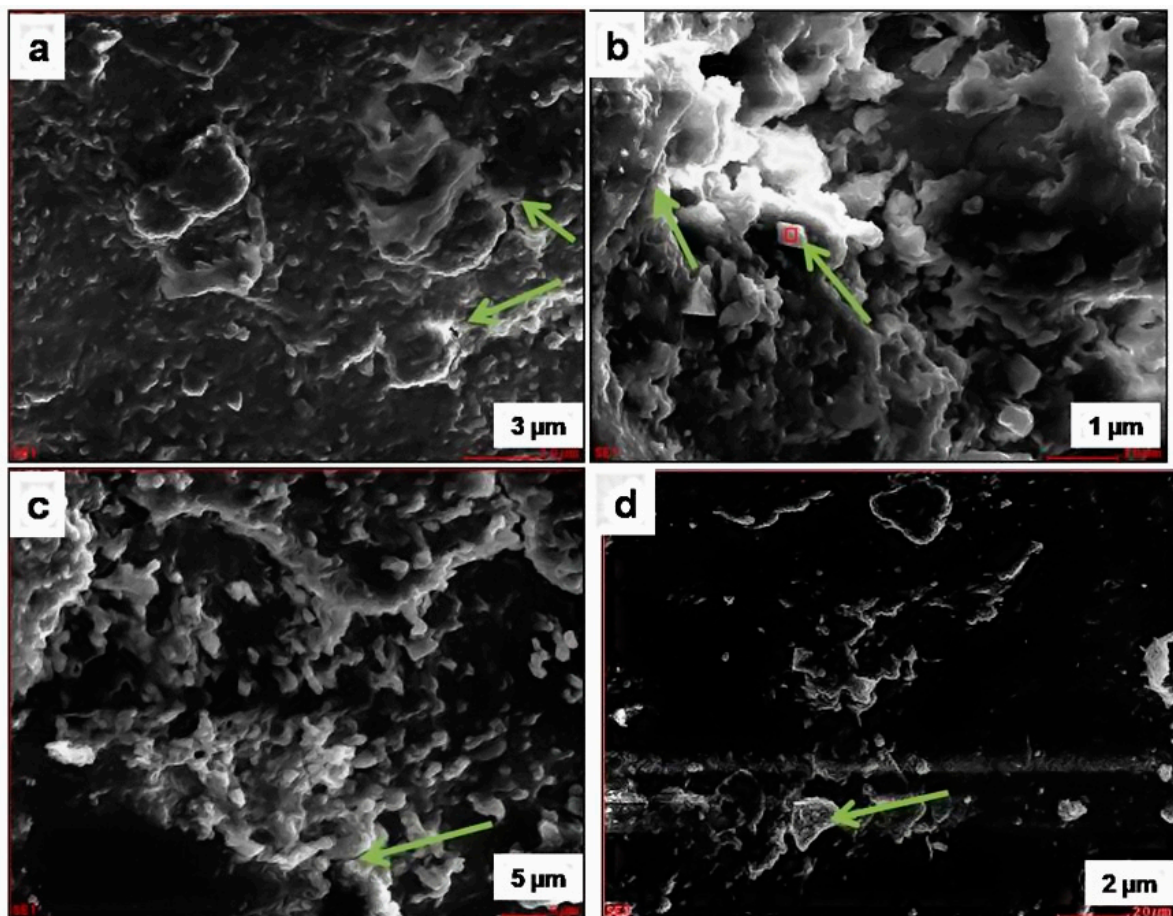


Figure 10. SEM image of the deteriorated stone sample: (a) arrow shows quartz; (b) arrow shows plagioclase feldspar with K-feldspar overgrowths; (c) arrow shows Mica-Biotite; (d) arrow shows Mica-Biotite.

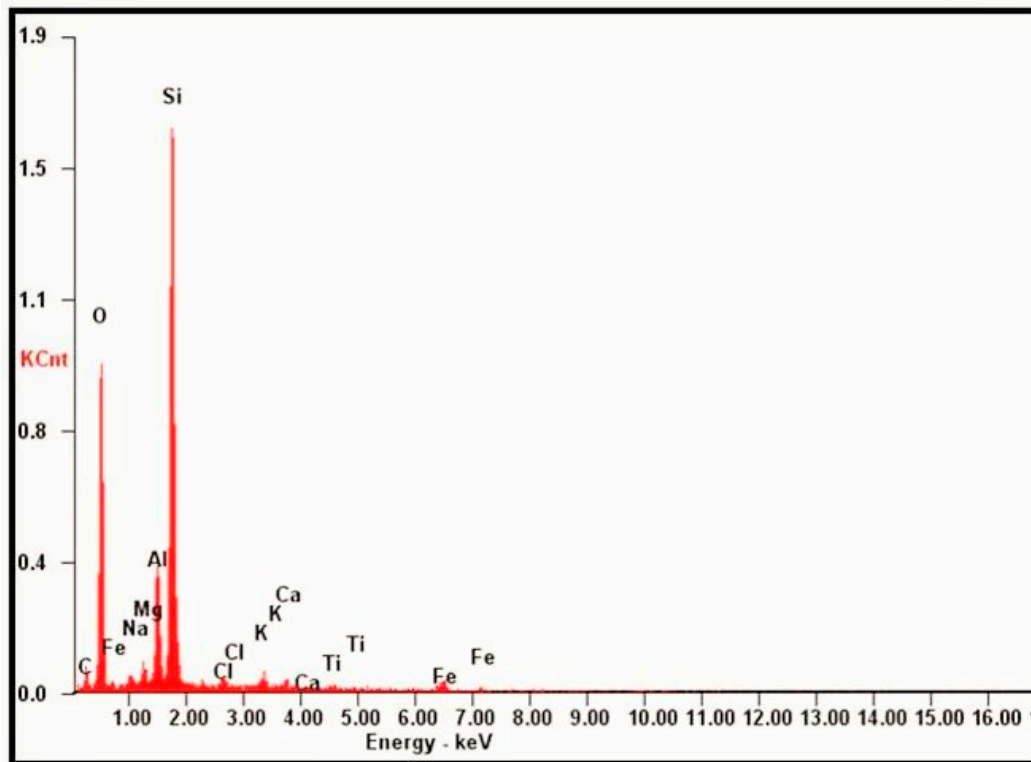


Figure 11. The representative SEM-EDX spectrum.

Authigenic quartz overgrowths partly filling pores between detrital quartz grains were also observed from the SEM images. The overgrowth grew against a pore wall, and the authigenic quartz molded itself around the druse-lined detrital grain (arrow; Figure 10a), forming the texture seen in the SEM image. From the SEM photomicrographs of the deteriorated sample, it was clear that the presence of crystallization of the minerals and salt efflorescence (Figure 10b) was evidenced. The quartz may be attributed to the resultant products of the deterioration of the stone samples due to weathering caused by the salt-laden winds from the sea. The results correlated with the chemical composition of the samples.

3.5. Analysis of Lime Plaster

As already stated, the monument may have been lime plastered in the past as a protective layer that has now diminished. Only the profile remains in the shelter area, as well as a few sculptures. The sculpture with remnants of historical plasters is still in a good state of conservation despite the adverse climatic condition. Thermal analysis graph DTA/TGA is shown in Figure 12.

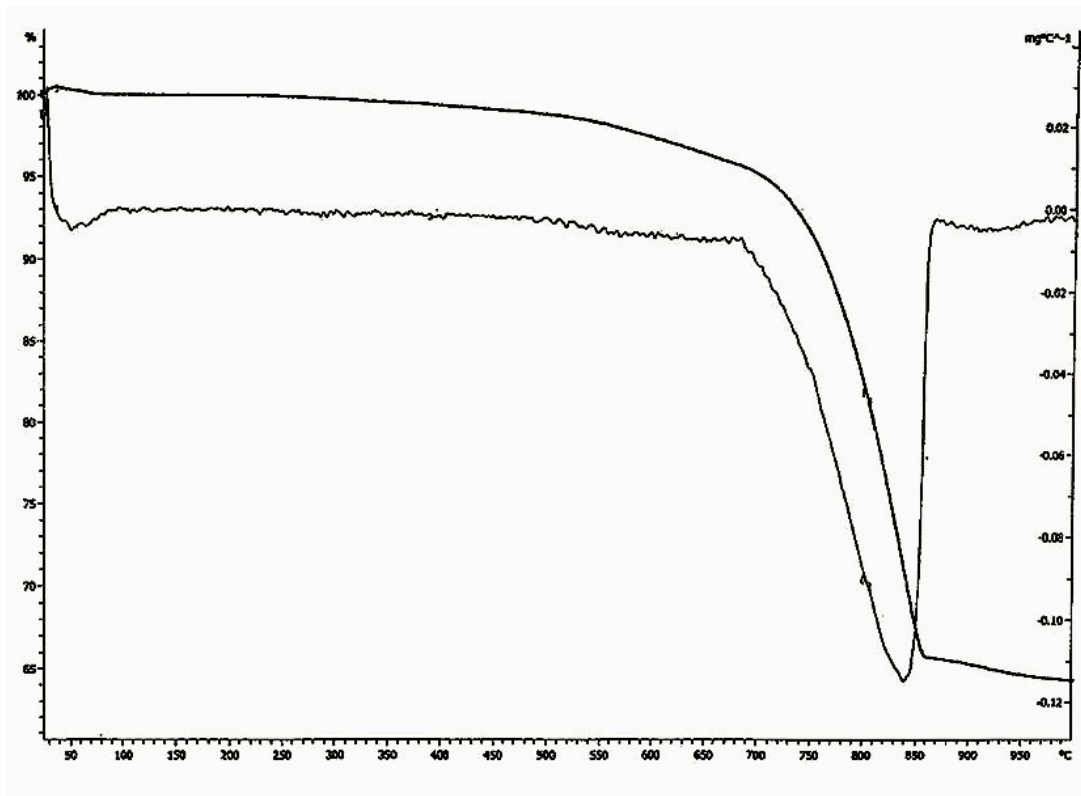


Figure 12. Thermo gravimetric analysis (TGA)—differential thermal analysis (DTA) diagram of lime plaster of Shore Temple, Mahabalipuram.

In the thermo gravimetric (TG) curve, the continuous weight loss was observed between the temperature range of 700 °C to 840 °C for the sample. Since the temperature of decomposition of calcium carbonate depends on its crystallinity, this suggests that part of the binder was perfectly crystalline. As pure calcium carbonate decomposes at 840 °C, the lime used for the plaster preparation of Shore Temple might have been an aerial lime of high purity. From the particle size analysis of the lime plaster (Figure 13), it was observed that the size of the aggregates used for the plaster was in the range of 1 μm to 700 μm . The majority of the aggregates were in the size range of 100 μm to 500 μm , which denotes that the aggregates used in the preparation of the plaster were mostly uniform in size. From the thermal analysis data, it was observed that the plaster of the temple was a non-hydraulic lime of high purity.

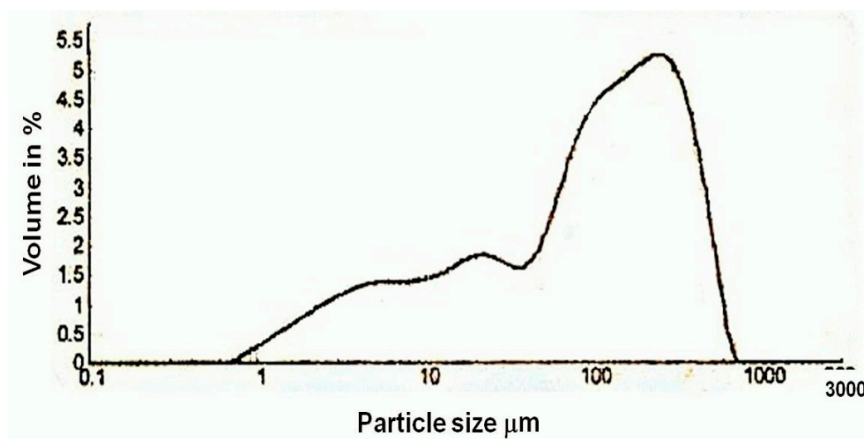


Figure 13. Particle size analysis diagram of lime plaster of Shore Temple, Mahabalipuram.

The chemical analysis results for two numbers of lime plasters are shown in Table 4. From the chemical composition, it can be seen that there was a high percentage of CaO and that the plaster was binder rich.

Table 4. Chemical composition of lime plaster samples of Shore Temple, Mahabalipuram.

Sample No.	Moisture	Organic Matter	LOI *	Acid Insoluble Residue Mostly Silica SiO ₂	R ₂ O ₃	CaO	MgO	Total
Sample No.1	1.30	2.75	26.08	36.38	3.49	26.60	3.2	99.80
Sample No.2	2.14	4.48	16.96	52.48	1.95	21.56	0.40	99.95

* LOI—Loss on ignition.

The plasters and renders made up of non-hydraulic lime are easily susceptible to deterioration caused by salts [40]. Lime rendering on wet and salt contaminated walls may show discoloration, moisture stains, salt efflorescence, and strong banding [43]. The rendering made of high calcium lime often shows accelerated weathering in a short time, as they are mostly used as a protective layer. The lime rendering previously applied to the temple worked as a protective layer, protecting the surface of high aesthetic value from deterioration by salt crystallization for a limited period of time. After its detachment and loss from the temple stone surface, the monument was left to bear the onslaught of adverse climatic conditions, as no attempt was made for re-rendering the plaster, resulting in extensive deterioration of the sculptures and the surface. The stone surfaces with remnants of plasters are still in a good state and remain free from any damage.

3.6. Conservation Treatment

3.6.1. Paper Pulp Treatment

The results on conductivity data of the paper pulp applied to both the exterior and the interior areas of the southern prakara wall of the temple versus the number of applications of poultices is shown in Figure 14. The specific conductivity decreased with an increase in the application of paper pulp (Table 5). From Figure 14, it was observed that the decrease in the chloride content was quite considerable to the fifth application of paper pulp, and thereafter it was not. From Figure 14, it was also observed that cellulose-based poultices were able to remove about 70% of salts in the humid environment of Mahabalipuram. Complete removal is rather difficult. Moreover, replenishment of the salts on the stone surface occurred due to sea sprays. Figure 15 shows a view of the temple during paper pulp treatment. Six to eight applications of paper pulp were carried out to achieve the desired results. The effectiveness of this treatment was also tested by carrying out conductivity measurements of the aqueous extract of the paper pulp.

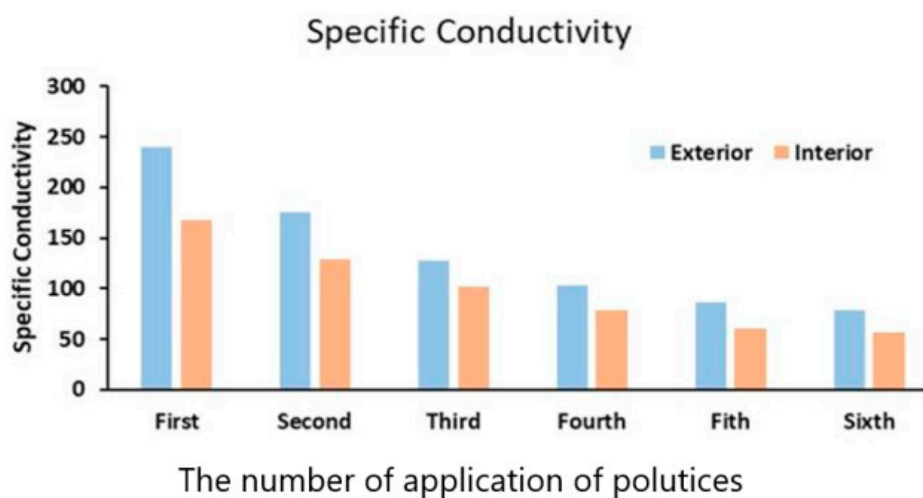


Figure 14. Specific conductivity ($\mu\Omega \text{ cm}^{-1}$) of the aqueous extract extracted from the Shore Temple by several applications of paper pulp.



Figure 15. The photograph showing the paper pulp poultice application at the Shore Temple, Mahabalipuram.

Table 5. Specific conductivity ($\mu\Omega \text{ cm}^{-1}$) of the aqueous extract extracted from the Shore Temple by several applications of paper pulp.

No. of Application	Exterior	Interior
First	240	167
Second	175	129
Third	128	102
Fourth	103	78
Fifth	86	61
Sixth	78	56

The results were characterized by an increase in total dissolved solids (TDS) of water used for washing paper pulp. The chloride content of the aqueous extract came to a lower value one week after paper pulp treatment. However, the enrichment of TDS in the poultices applied on stone surfaces was only due to the salts still present in the pores of the stone. This showed that the complete removal of salts from the stone surface is nearly impossible. Moreover, enrichment of surfaces with the sea sprays was again noticed after two to three weeks of the poultices application. This indicates that regardless of the methodology applied for the extraction of salts using different types of poultices on the basis of pore size and pore diameter of granitic stone, the surface enriches quickly with saline salts due to climatic conditions prevailing at Mahabalipuram.

3.6.2. The Efficiency of Poultice Treatment

In the present study, the chloride content of paper pulp applied on both exterior and interior surfaces of a western panel of the monument was estimated, and the results are shown in Figure 16. The graph of chloride percentage versus a number of applications of paper pulp shows that the repeated application of paper pulp considerably reduced the concentration of salts, but the salt content could not be reduced beyond a certain point despite repeated applications. A nearly straight line in Figure 14 suggests that the cost of application of paper pulp would be very high if it continued beyond the fifth time. After the application of poultices treatment, the granitic stone turned to its original texture and color—on a limited scale. However, a constant spray of salts from the sea again replenished the salts, and the stone returned to its original condition.

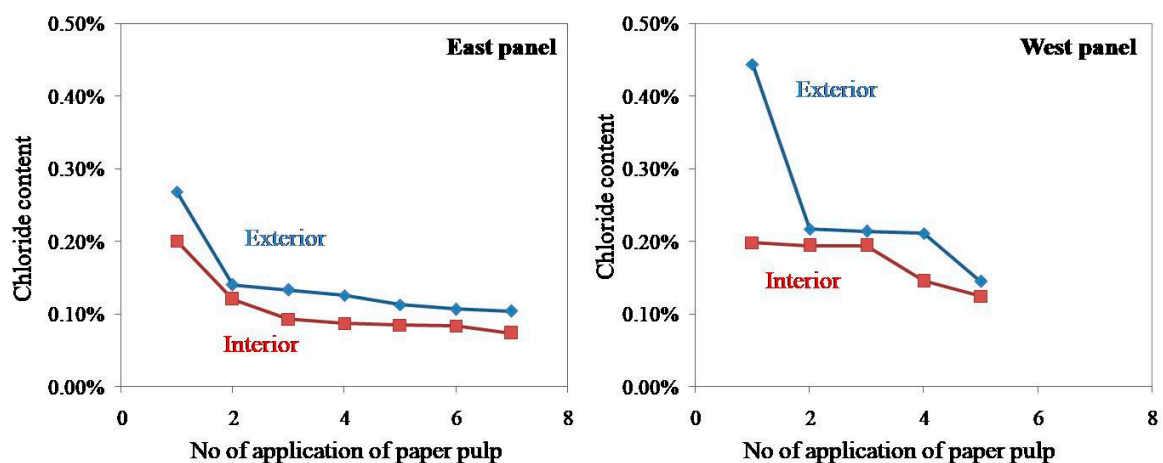


Figure 16. The graph of chloride percentage against a number of applications of paper pulp.

From the onsite study of the distribution of sea salts in the granite stone of Shore Temple having a porosity mostly between 0.5 to 1.5%, it was observed that salts were mostly concentrated in a millimeter thin film on the surface of the stone and caused considerable damage. Salt reduction by application of poultices is usually the best method of desalination, as it only affects a few centimeters of the substrate. In most cases, cellulose fibers or a mixture of clay and aggregates with or without cellulose fibers are used for poultices. The specific requirement for the poultices is as follows: it must be very water absorbent; it should retain water to a certain extent to regulate evaporation velocity; it should have a high specific surface area and a high exchange capacity to absorb a maximum quantity of salts. It has been observed that poultices containing clay minerals have higher efficacy than those containing only cellulose fibers. The porosity obtained through the cellulose fibers is not sufficient to guarantee complete diffusion of salts from the substrate with pores smaller than 15 μm , i.e., no advection will occur on the smallest pores present in granite. This points out how the practice of desalination of the object based on cellulose poultices is far from achieving the desired results. However, the poultices made up of cellulose fibers have an advantage; they can be applied on fragile

surfaces like Mahabalipuram granite stone since they are soft, easy to handle, and can be removed from most of the surface without any residue. Applying cellulose-based paste four to five times eliminated most of the salts from the stone surface, but there was no complete desalination. One of the advantages of cellulose-based poultices is that there are no new materials introduced in the substrate except water. The efficiency of desalination can be evaluated by considering the percentage of salts removed [44]. For cellulose-based poultices, keeping the poultices longer will also attract mold growth. Also, the limited shrinkage of the poultices in humid conditions apparently leads to fewer poultices being detached, which is often the case. The results of the poultices efficacy are between 50 to 70% [45].

This efficiency directly depends on the adhesion of poultices to the substrate, the drying cycle, and the length of treatment. Desalinating masonry in a humid environment led to leaving the poultices for months instead of weeks [46]. A higher number of cellulose poultices applications could increase the efficiency of desalination, but there is no guarantee of total extraction of salts. Poultices shrink as they dry and may detach from the wall. At this point, they cease to extract moisture and salts [47]. As the surface of the granite stone of the temple is already very deteriorated, it was sometimes observed that the part of the surface stone that lost cohesiveness was removed along with the dried poultices. At all such surfaces—where the stone surface was pulverized—an intermediate layer of Japanese tissue paper was applied over the stone, followed by the application of cellulose poultices. After temporary salt reduction, the stone strengthening by silicic acid ester was carried out for the temple before the salt content was replenished.

4. Discussion

At Shore Temple, Mahabalipuram, it was observed that salt reduction from the stone surface is only temporary, and necessary conservation measures must be initiated instantly before the salt content is replenished due to a continuous spray of sea salts. The crystalline inhibitors such as salt transporting or salt accumulating materials that favor salt crystallization at the surface (efflorescence) were also considered for application on the stone surface, but it was disallowed due to health and environmental reasons [48] and the continuous feeding of sea sprays to the monument.

After the temporary salt reduction, the stone strengthening by silicic acid ester was carried out for the temple before the salt content was replenished. However, the formation of silica was hampered by the high salt content and the increased solar radiation, which sped up the degradation of the water repellent coating [49,50]. The negatives of silicone consolidants is that they are more fragile, less elastic, and can be damaged due to salt crystallization [49,50]. The mechanical stress due to sandblasting on the surface might have produced a creep, and the consolidant could no longer improve cohesiveness among the components of the damaged materials, thus the damage continued. As already stated, the Shore Temple was treated with a protective layer of lime plaster, traces of which were observed in the shelter area. This non-hydraulic lime had very high porosity with larger pore sizes in comparison with the porosity of the stones. From close observation of the plaster, two layers of rendering were seen, and the upper one had small pores of a water repellent admixture. The functional principle of the render was that the salt solution slowly entered the interior part of the rendering and accumulated at the contact point of the upper layer. Water evaporated and escaped through water vapor diffusion while the salt crystallized in large pores of the render. Consequently, the surface of the render remained dry and free of salt efflorescence or new damage. The cementitious binding lime made the render insensitive to salt crystallization. These renders successfully worked at Shore Temple, Mahabalipuram until it was saturated with salts and disfunction falling from the stone surfaces. The monument was no longer treated with similar renders, and damage to the now exposed granitic stone continued. The surface was lost and the sculptures were obliterated.

As the temple stands on the threshold of the sea, it is not only combating the injurious effects of saline action due to sprays of seawater but also the onslaught of sandblasting caused by the high-velocity winds carrying sand particles. Several years ago, the sea waves were actually lashing the walls of the temple on the eastern side. At the times of the full moon and the new moon, the high tides used to enter the corridor of the temple. The groyne wall was a massive, newly constructed wall to serve as protection from waves. It was built in stone and concrete blocks to protect the temple from lashing waves and keep the sea a little further away. As the groyne wall was not very efficient in stopping the sea waves, boulders were brought from elsewhere and dumped massively in the sea. The giant wave of the 26 December 2004 tsunami smashed the groyne wall (built in 1970), tore down the fence, flooded the lawns, and entered the Shore Temple. Some structures and rocks, perhaps components of the complex of which the Shore Temple was originally a part, came into view when the sea initially receded from the shoreline. The waves dislocated the foundation of the protective alter in front of Shore Temple [51]. However, the original temple survived, as it was built on bedrock.

To save the great identity of the Pallava ruler on the seashore, the groyne wall that was damaged in the tsunami should be strengthened and made much more effective in saving Shore Temple from sea tides. There is a need to cut wind velocity by increasing forestation between the temple and the sea, specifically casuarina trees. The gardening that was done all around the monument has helped in the conservation of the stone surface by reducing the sandblasting. The ethyl silicate consolidation carried for the temple after desalination no longer saves the monument from further damage. It is advisable that compatible lime render be applied as a protective layer to save the historic surfaces from further damage.

5. Conclusions

Marine salts and sand-laden winds are the main causes of deterioration of Shore Temple. The high precipitation and wind-driven rain led to the penetration of sea salts, consequently causing hygric expansion with accompanying stress to the granitic gneiss. The high humidity and dampness stimulated the minerals to undergo hydrolysis. The petrological analysis shows potash aluminosilicate of the rock, indicating that orthoclase and microcline hydrolyzed. The biotite and feldspar altered to a different degree from west to east. Alumina enriched in heavily deteriorating stone, which was accompanied by the depletion of SiO_2 . The chemical reaction accelerated the flaking of the stone surface and the sand-laden wind dislodged the loosely adhered stone particles. As the monument is continuously exposed to wind and salt deposition, the honeycomb weathering (alveolarization) has formed on the stone surface. The sides of the temple that face the sea and the upper part of the temple currently show intense alveolarization. The high temperatures and high precipitation have also caused bio-colonization. The application of cellulose-based poultices four to five times removed most of the salts from the stone surface, but there is no complete desalination. Replenishment of salt on the stone surface occurs often due to continuous sea sprays. The silicon stone strengthener applied in the past did not work due to high humidity and UV radiation. It was also damaged by salt crystallization, as it is more fragile and less elastic. To save the lone Pallava temple on the seashore, compatible non-hydraulic lime rendering that is still evidenced in the shelter area may have to be applied as a sacrificial layer. The groyne wall damaged in the massive 2004 tsunami should be strengthened and made more effective. There is a need for increased afforestation to cut wind velocity.

Author Contributions: Both the Authors contributed equally to this research work.

Funding: This research received no external funding.

Acknowledgments: The author (M.R.S.) is thankful to the B. R. Mani, Vice-Chancellor, National Museum Institute, New Delhi for his support and interest in the work. The authors are thankful to Tahseen Karche and Bhushan Dighe Research scholars, National Museum Institute. We are thankful to the Director General, ASI, New Delhi and the Director (Science), ASI, Dehradun for all their Support. The authors are also thankful to Sh. Busa Goud Bhashyam, Dy. SAC, Sh. Manivannan, AAC, Sh. Prasobhraj, AAC and Remyaraj, AAC of ASI, Science Branch, Chennai.

Conflicts of Interest: The authors declare no conflict of interest.

References

- Schaffer, R. *The Weathering of Natural Building Stone*; Routledge: Abingdon, UK, 2016.
- Lewin, S.Z. The Mechanism of Masonry Decay through Crystallization. In *Conservation of Historic Stone Building and Monuments*; National Academy of Sciences: Washington, DC, USA, 1982; pp. 120–144.
- Sabbioni, C.; Cassar, M.; Brimblecombe, P.; Tidblad, J.; Kozłowski, R.; Drdácáký, M. *Global Climate Change Impact on Built Heritage and Cultural Landscapes*; Taylor & Francis Ltd.: Milton Park, UK, 2006.
- Lubelli, B. *Sodium Chloride Damage to Porous Building Materials*; University of Technology: Delft, The Netherlands, 2006.
- Luquer, L.M. *The Relative Effects of Frost and the Sulfate of Soda Efflorescence Tests on Building Stones*; Columbia University: New York, NY, USA, 1985.
- Taber, S. The growth of crystals under external pressure. *Am. J. Sci.* **2018**, *41*, 532–556. [[CrossRef](#)]
- Jutson, J.T. The influence of salts in rock weathering in sub-arid western Australia. *Proc. R. Soc. Vic.* **1918**, *30*, 165–172.
- Smith, B.J. Weathering Processes and Forms. In *Geomorphology of Desert Environments*; Parsons, A.J., Abrahams, A.D., Eds.; Springer: Dordrecht, The Netherlands, 2009; pp. 69–100. [[CrossRef](#)]
- Nash, D.J. Arid geomorphology. *Prog. Phys. Geogr. Earth Environ.* **2000**, *24*, 425–443. [[CrossRef](#)]
- Lubelli, B.; Cnudde, V.; Diaz-Goncalves, T.; Franzoni, E.; van Hees, R.P.J.; Ioannou, I.; Menendez, B.; Nunes, C.; Siedel, H.; Stefanidou, M.; et al. Towards a more effective and reliable salt crystallization test for porous building materials: State of the art. *Mater. Struct.* **2018**, *51*, 55. [[CrossRef](#)]
- Sallam, E.S.; El-Aal, A.K.A.; Fedorov, Y.A.; Bobrysheva, O.R.; Ruban, D.A. Geological heritage as a new kind of natural resource in the Siwa Oasis, Egypt: The first assessment, comparison to the Russian South, and sustainable development issues. *J. Afr. Earth Sci.* **2018**, *144*, 151–160. [[CrossRef](#)]
- Grementieri, L.; Daghia, F.; Molari, L.; Castellazzi, G.; Derluyn, H.; Cnudde, V.; Miranda, S. A multi-scale approach for the analysis of the mechanical effects of salt crystallisation in porous media. *Int. J. Solids Struct.* **2017**, *126*, 225–239. [[CrossRef](#)]
- Desarnaud, J.; Derluyn, H.; Grementieri, L.; Molari, L.; de Miranda, S.; Cnudde, V.; Shahidzadeh, N. Salt contaminated sandstone under environmental loading: Recrystallization process and its consequences. In Proceedings of the International RILEM Conference on Materials, Systems and Structures in Civil Engineering—Segment on Historical Masonry, Kgs. Lyngby, Denmark, 22–24 August 2016; RILEM Publications: Kgs. Lyngby, Denmark, 2016; pp. 127–136.
- Derluyn, H.; Moonen, P.; Carmeliet, J. Deformation and damage due to drying-induced salt crystallization in porous limestone. *J. Mech. Phys. Solids* **2014**, *63*, 242–255. [[CrossRef](#)]
- Koniorczyk, M.; Gawin, D. Modelling of salt crystallization in building materials with microstructure—Poromechanical approach. *Constr. Build. Mater.* **2012**, *36*, 860–873. [[CrossRef](#)]
- Coussy, O. Deformation and stress from in-pore drying-induced crystallization of salt. *J. Mech. Phys. Solids* **2006**, *54*, 1517–1547. [[CrossRef](#)]
- Thompson, J. *The Disintegration of Stones Exposed in Buildings and Otherwise to Atmospheric Influence*; Report of the Annual Meeting; British Association for the Advancement of Science: London, UK, 1862; p. 257.
- Scherer, G.W. Crystallization in pores. *Cem. Concr. Res.* **1999**, *29*, 1347–1358. [[CrossRef](#)]
- Zezza, F.; Macri, F. Marine aerosol and stone decay. *Sci. Total Environ.* **1995**, *167*, 123–143. [[CrossRef](#)]
- Moropoulou, A.; Theoulakis, P.; Chrysophakis, T. Correlation between stone weathering and environmental factors in marine atmosphere. *Atmos. Environ.* **1995**, *29*, 895–903. [[CrossRef](#)]
- Mustoe, G. The Origin of honeycomb weathering. *Geol. Soc. Am. Bull.* **1982**, *93*, 108–115. [[CrossRef](#)]
- Grisez, L. Coastal alveolization of metamorphic schist. *Dyn. Geomorphol. Rev.* **1960**, *11*, 164–167.
- Goudie, A.S.; Viles, H.A. *Salt Weathering Hazards*; Wiley: Hoboken, NJ, USA, 1997.
- Trenhaile, A.S. *The Geomorphology of Rocky Coast*; Oxford University Press: Oxford, UK, 1987.

25. Prebble, M.M. Cavernous Weathering in the Taylor Dry Valley, Victoria Land, Antarctica. *Nature* **1967**, *216*, 1194. [[CrossRef](#)]
26. Dragovich, D. Building Stone and Its Use in Rock Weathering Studies. *J. Geol. Educ.* **1979**, *27*, 21–25. [[CrossRef](#)]
27. Rodriguez-Navarro, C. Evidence of honeycomb weathering on Mars. *Geophys. Res. Lett.* **1998**, *25*, 3249–3295. [[CrossRef](#)]
28. Stierlin, H. *Hindu India: From Khajuraho to the Temple City of Madurai*; Taschen America LLC: Cologne, Germany, 1998.
29. Spennemann, D.H.R.; Pike, M.; Watson, M.J. Effects of acid pigeon excreta on building conservation. *Int. J. Build. Pathol. Adapt.* **2017**, *35*, 2–15. [[CrossRef](#)]
30. Spennemann, D.H.R.; Pike, M.; Watson, M.J. Bird impacts on heritage buildings: Australian practitioners' perspectives and experiences. *J. Cult. Herit. Manag. Sustain. Dev.* **2018**, *8*, 62–75. [[CrossRef](#)]
31. Spennemann, D.; Pike, M.; Watson, M. Behaviour of Pigeon Excreta on Masonry Surfaces. *Restor. Build. Monum.* **2018**, *23*, 15–28. [[CrossRef](#)]
32. Dyer, T. Deterioration of stone and concrete exposed to bird excreta—Examination of the role of glyoxylic acid. *Int. Biodeterior. Biodegradation.* **2017**, *125*, 125–141. [[CrossRef](#)]
33. ISO 7888-1985 (E). *Water Quality—Determination of Electrical Conductivity Qualit&' de L'eau—Determination de la Conduc Tivitd Blec Trique First Edition*; ISO: Geneva, Switzerland, 1985.
34. ISO 9297-2000. *Water Quality—Determination of Chloride—Silver Nitrate Titration with Chromate Indicator (Mohr's Method)*; Hach Company/Hach Lange GmbH: Loveland, CO, USA, 2014–2015.
35. Nairn, A.E.M.; Stehli, F.G. *The Ocean Basins and Margins: The South Atlantic*; Springer: London, UK, 1973.
36. Chester, R.; Jickells, T.D. *Marine Geochemistry*; John Wiley & Sons: Hoboken, NJ, USA, 2012.
37. Auras, M. Poultrices and mortars for salt contaminated masonry and stone objects. In *Salt Weathering on Buildings and Stone Sculptures, Proceedings of the International Conference*; Technical University of Denmark: Copenhagen, Denmark, 2008; pp. 197–217.
38. Köppen, W. Die Wärmezonen der Erde, nach der Dauer der heissen, gemässigten und kalten Zeit und nach der Wirkung der Wärme auf die organische Welt betrachtet. *Meteorol. Zeitschrift.* **1884**, *1*, 5–226.
39. Rubel, F.; Kottke, M. Comments on: "The thermal zones of the Earth" by Wladimir Köppen (1884). *Meteorol. Zeitschrift.* **2011**, *20*, 361–365. [[CrossRef](#)]
40. Graue, B.; Siegesmund, S.; Middendorf, B. Quality assessment of replacement stones for the Cologne Cathedral: Mineralogical and petrophysical requirements. *Environ. Earth Sci.* **2011**, *63*, 1799–1822. [[CrossRef](#)]
41. Carroll, D.; Starkey, H.C. Effect of sea-water on clay minerals. In *Clays and Clay Minerals, Proceedings of the Seventh National Conference, Washington, DC, USA, 20–23 October 2013*; Permagon Press: Oxford/London, UK; pp. 80–101.
42. Hoppert, M.; Flies, C.; Pohl, W.; Günzl, B.; Schneider, J. Colonization strategies of lithobiontic microorganisms on carbonate rocks. *Environ. Geol.* **2004**, *46*, 421–428. [[CrossRef](#)]
43. Hendry, E.A. Masonry walls: Materials and construction. *Constr. Build. Mater.* **2011**, *15*, 323–330. [[CrossRef](#)]
44. Saidov, T.; Pel, L.; Kopinga, K. Sodium sulfate salt weathering of porous building materials studied by NMR. *Mater. Struct.* **2017**, *50*, 1–11. [[CrossRef](#)]
45. Domasłowski, M.; Kęsy-Lewandowska, W. Wpływ warunków odsalania kamienia efektywność usuwania soli. *Acta Univ. Nicolai Copernici. Nauk. Humanist. Zabytkozn. Ikonsertw.* **1998**, *30*, 59–71.
46. Doehne, E.; Schiro, M.; Roby, T.; Chiari, G.; Lambousy, G.; Knight, H. Evaluation of poultice desalination process at Madame Johns' Legacy, New Orleans. In *Proceedings of the 11th International Congress on Deterioration and Conservation of Stone, Torun, Poland, 15–20 September 2008*; pp. 857–864.
47. Vergès-Belmin, V.; Siedel, H. Desalination of Masonries and Monumental Sculptures by Poulticing: A Review/Entsalzen von Mauerwerk und Steinfiguren mit Hilfe von Kompressen: Ein Überblick, *Restor. Build. Monum.* **2005**, *11*, 391–408. [[CrossRef](#)]
48. Rivas, T.; Alvarez, E.; Mosquera, M.; Alejano, L.; Taboada, J. Crystallization modifiers applied in granite desalination: The role of the stone pore structure. *Constr. Build. Mater.* **2010**, *24*, 766–776. [[CrossRef](#)]
49. Sandrolini, F.; Elisa, F.; Barbara, P. Ethyl silicate for surface treatment of concrete—Part I: Pozzolanic effect of ethyl silicate. *Cem. Concr. Compos.* **2012**, *34*, 306–312. [[CrossRef](#)]

50. Franzoni, E.; Gabriela, G.; Enrico, S.; Ginevra, B.; Michele, G.; Pietro, L. Solvent-based ethyl silicate for stone consolidation: Influence of the application technique on penetration depth, efficacy and pore occlusion. *Mater. Struct.* **2015**, *48*, 3503–3515. [[CrossRef](#)]
51. Subramanian, T. *The Shore Temple Stands Its Ground*; The Hindu: Chennai, India, 2004.



© 2019 by the authors. Licensee MDPI, Basel, Switzerland. This article is an open access article distributed under the terms and conditions of the Creative Commons Attribution (CC BY) license (<http://creativecommons.org/licenses/by/4.0/>).